Inorganica Chimica Acta 370 (2011) 420–426

Contents lists available at ScienceDirect

Inorganica Chimica Acta

journal homepage: www.elsevier.com/locate/ica

Intramolecular ether oxygen coordination in the zinc complexes with dipicolylamine (DPA)-derived ligands

Yuji Mikata [a,*], Tomomi Fujimoto [b], Tomomi Fujiwara [b], Shin-ichi Kondo [c]

[a] KYOUSEI Science Center, Faculty of Science, Nara Women's University, Nara 630-8506, Japan
[b] Department of Chemistry, Faculty of Science, Nara Women's University, Nara 630-8506, Japan
[c] Department of Material and Biological Chemistry, Faculty of Science, Yamagata University, Yamagata 990-8560, Japan

ARTICLE INFO

Article history:
Received 8 July 2010
Received in revised form 4 February 2011
Accepted 9 February 2011
Available online 16 February 2011

Keywords:
Zinc complex
Coordination mode
Ligand effect
Ether oxygen

ABSTRACT

The ether oxygen coordination to the zinc center in the complexes with dipicolylamine (DPA)-derived ligands, *N*-(2-methoxyethyl)-*N*,*N*-bis(2-pyridylmethyl)amine (**L**), *N*-(3-methoxypropyl)-*N*,*N*-bis(2-pyridylmethyl)amine (**L′**), and *N*-{3-(2-pyridylmethyloxy)propyl}-*N*,*N*-bis(2-pyridylmethyl)amine ($\mathbf{L}^{\mathbf{Py}}$) has been discussed. Upon chelation of the oxygen atom, **L** forms a five-membered chelate ring with respect to the 2-aminoethyl ether moiety whereas **L′** forms a six-membered chelate in 3-aminopropyl ether unit. This difference was highlighted by the crystal structures of $ZnCl_2$ complexes, in which [Zn(**L**)Cl_2] (**1**) exhibited ether oxygen coordination but [Zn(**L′**)Cl_2] (**2**) had the ether oxygen non-coordinated. The terminal pyridyl group of $\mathbf{L}^{\mathbf{Py}}$ facilitates the ether oxygen atom coordination via a metal binding from the basal plane *trans* to the aliphatic nitrogen.

1. Introduction

Binding of ether oxygen atom to the metal center is commonly found in metal complex structures. Represented by the crown ethers, this single metal–oxygen bond is moderate to weak in strength, however, cooperative binding by accumulating weak interactions makes metal–ether oxygen bonds strong and specific [1–4]. Tethering of ether moiety with strong metal binding site is another effective method to facilitate the ether oxygen coordination to the metal center [2,3]. This chelation effect becomes maximal when five-membered ring is formed. The six-membered chelate structures are also commonly used.

Dipicolylamine (2,2′-dipyridylmethylamine, DPA) is one of the most studied tridentate metal-binding units in the coordination chemistry [5–9]. As described above, linking an ether pendant chain to the DPA moiety would enhance the ether oxygen binding to the metal center [10]. Strong binding of the DPA unit to the copper(II) [5–9,11] assists the coordination of the anomeric oxygen atom of the sugar unit to the metal center, generating an asymmetric oxygen [12,13]. Similar idea for the improvement of ether oxygen coordination was employed by Sigel using a phosphate group in place of DPA [14,15]. With this respect, here we prepared zinc complexes with a DPA-pendant ether ligand to evaluate the intramolecular metal-coordination ability of oxygen atom in solid and solution state. Zinc plays a lot of important roles in biological processes [16,17]. Thus, a lot of fluorescent zinc sensor molecules having DPA unit as a zinc-binding site have been reported [18–21]. Multidental nitrogen and oxygen ligands bound to zinc center have been investigated within the field of bioinorganic chemistry [22–24]. Zinc–DPA complex is also used as model complexes of hydrolytic enzymes of phosphate esters including nucleic acids [25,26]. Bis(Zn–DPA) unit is utilized for phosphate binding motif of fluorescent probe molecules for phosphate anions [27], pyrophosphates [28,29], nucleoside polyphosphates [30], and phosphoproteins [31].

The present ligand library includes **L** with aminoethyleneoxy moiety that forms five-membered chelate ring, **L′** with aminopropyleneoxy moiety that forms six-membered chelate ring, and $\mathbf{L}^{\mathbf{Py}}$ having aminopropyleneoxy and 2-pyridylmethyloxy moieties at the same ether oxygen atom, spawning six- and five-membered chelate upon metal binding (Chart 1). The structures of zinc complexes with these ligands were investigated by X-ray crystallography and ^{1}H NMR spectroscopy. The ligand structure as well as anion of the metal salt controls the ether oxygen coordination to the zinc center in these complexes.

2. Experimental

2.1. General

2.1.1. Equipments

Solvents and reagents used for the preparative procedures were obtained from commercial sources. ^{1}H NMR (300.07 Hz) and ^{13}C

* Corresponding author. Tel./fax: +81 742 20 3095.
E-mail address: mikata@cc.nara-wu.ac.jp (Y. Mikata).

0020-1693/$ - see front matter © 2011 Elsevier B.V. All rights reserved.
doi:10.1016/j.ica.2011.02.022

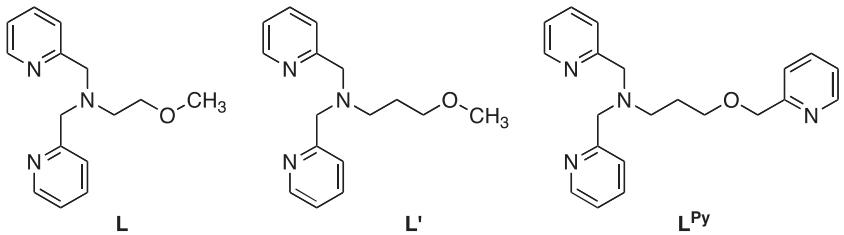

Chart 1.

(75.45 Hz) NMR spectra were recorded on a Varian GEMINI 2000 spectrometer and referenced to internal TMS or solvent signals. Elemental analyses were recorded on J-Science JM-10 micro corder. X-ray crystallography was performed on a Rigaku Mercury CCD system.

2.1.2. Materials

N-(2-methoxyethyl)-*N*,*N*-bis(2-pyridylmethyl)amine (**L**) [32] and *N*-(3-methoxypropyl)-*N*,*N*-bis(2-pyridylmethyl)amine (**L′**) [32] were prepared from 2-chloromethylpyridine and corresponding amines and characterized by ^{1}H and ^{13}C NMR spectroscopies. *Caution:* Perchlorate salts of metal complexes with organic ligands are potentially explosive. All due precautions should be taken.

2.2. Synthesis

2.2.1. *N*-{3-(2-pyridylmethyloxy)propyl}-*N*,*N*-bis(2-pyridylmethyl)amine (**L^{Py}**)

Anhydrous tetrahydrofuran solution of 3-hydroxypropyl-*N*,*N*-bis(2-pyridylmethyl)amine [5] (563 mg, 2.19 mmol) was added 1.78 mL (2.85 mmol) of *n*-butyllithium in hexane solution (1.6 M) at 0 °C, and the resulting red solution was stirred for 20 min. Then, 2-chloromethylpyridine (364 mg, 2.85 mmol) in tetrahydrofuran (10 mL) was added dropwise and the reaction mixture was stirred at 0 °C for 30 min, at room temperature for 1 h, and under reflux for 2 days. After cooled to room temperature, water was added and the organic material was extracted with chloroform. After removal of the solvent, the residual oily crude product was purified by column chromatography (Alumina, eluent: chloroform/methanol = 100/1) to afford *N*-{3-(2-pyridylmethyloxy)propyl}-*N*,*N*-bis(2-pyridylmethyl)amine (**L^{Py}**) as a brown oil (336 mg, 0.964 mmol, 44% yield). ^{1}H NMR ($CDCl_3$): δ 8.50–8.53 (m, 3H, py-6), 7.59–7.68 (m, 3H, py-4), 7.52 (d, J = 7.8 Hz, 2H, py-3), 7.31 (d, J = 7.8 Hz, 1H, py′-3), 7.10–7.19 (m, 3H, py-5), 4.56 (s, 2H, py′-CH_2–O), 3.83 (s, 4H, py-CH_2–N), 3.59 (t, J = 6.6 Hz, 2H, CH_2–O), 2.70 (t, J = 7.2 Hz, 1H, CH_2–N), 1.91 (m, 2H, C–CH_2–C). ^{13}C NMR ($CDCl_3$): δ 160.2, 159.1, 149.3, 136.9, 136.7, 123.2, 122.6, 122.2, 121.5, 74.0, 69.4, 60.8, 51.5, 27.8.

Anal. Calc. for $C_{21}H_{25}N_4O_{1.5}$ (**L^{Py}**·0.5H_2O): C, 70.56; H, 7.05; N, 15.67. Found: C, 70.98; H, 6.96; N, 15.60%.

2.2.2. Preparation of complexes

*2.2.2.1. [Zn(**L**)Cl$_2$] (**1**).* Methanolic solution (0.5 mL) of **L** (38.6 mg, 0.15 mmol) was mixed with $ZnCl_2$ (20.5 mg, 0.15 mmol) in the same solvent (0.5 mL) at room temperature. After 2 days, single crystals suitable for X-ray crystallography were obtained directly from the reaction mixture (21.5 mg, 0.055 mmol, 36% yield). Table 1 summarizes the crystallographic parameters.

^{1}H NMR (CD_3OD): δ 9.00 (d, J = 5.1 Hz, 2H, py-6), 8.11 (ddd, J = 1.8, 7.8, 7.8 Hz, 2H, py-4), 7.6–7.7 (m, 4H, py-3,5), 4.35 (s, 4H, py-CH_2–N), 3.16 (s, 3H, CH_3), 2.9–3.0 (m, 4H, CH_2CH_2).

^{13}C NMR (CD_3OD): δ 156.1, 149.1, 142.1, 125.8, 125.1, 68.4, 61.2, 59.1, 57.9.

Anal. Calc. for $C_{15}H_{19}Cl_2N_3OZn$ (**1**): C, 45.77; H, 4.87; N, 10.68. Found: C, 45.50; H, 4.79; N, 10.53%.

*2.2.2.2. [Zn(**L′**)Cl$_2$] (**2**).* Methanolic solution (1.0 mL) of **L′** (40.7 mg, 0.15 mmol) was mixed with $ZnCl_2$ (20.6 mg, 0.15 mmol) in the same solvent (1.0 mL) at room temperature. After 2 days, single crystals suitable for X-ray crystallography were obtained directly from the reaction mixture (44.5 mg, 0.11 mmol, 73% yield). Table 1 summarizes the crystallographic parameters.

^{1}H NMR (CD_3OD): δ 8.93 (d, J = 4.5 Hz, 2H, py-6), 8.16 (ddd, J = 1.5, 7.8, 7.8 Hz, 2H, py-4), 7.6–7.7 (m, 4H, py-3,5), 4.31 (s, 4H, py-CH_2–N), 3.29–3.39 (m, 2H, CH_2–O), 3.26 (s, 3H, CH_3), 2.81–2.87 (m, 2H, CH_2–N), 1.7–1.8 (m, 2H, C–CH_2–C).

^{13}C NMR (CD_3OD): δ 156.4, 149.7, 142.1, 125.9, 125.3, 71.5, 58.8, 58.4, 53.6, 25.6.

Anal. Calc. for $C_{16}H_{21}Cl_2N_3OZn$ (**2**): C, 47.14; H, 5.19; N, 10.31. Found: C, 46.71; H, 5.15; N, 10.18%.

*2.2.2.3. [Zn(**L′**)$_2$](ClO$_4$)$_2$ (**3**).* Methanolic solution (0.5 mL) of **L′** (27.1 mg, 0.10 mmol) was mixed with $Zn(ClO_4)_2$ (26.4 mg, 0.10 mmol) in the same solvent (0.5 mL) at room temperature. After 3 days, single crystals suitable for X-ray crystallography were obtained directly from the reaction mixture (16.4 mg, 0.020 mmol, 40% yield). Table 1 summarizes the crystallographic parameters.

Table 1
Crystallographic data for [Zn(**L**)Cl$_2$] (**1**), [Zn(**L′**)Cl$_2$] (**2**), and [Zn(**L′**)$_2$](ClO$_4$)$_2$ (**3**).

	[Zn(**L**)Cl$_2$] (**1**)	[Zn(**L′**)Cl$_2$] (**2**)	[Zn(**L′**)$_2$](ClO$_4$)$_2$ (**3**)
Formula	$C_{15}H_{19}Cl_2N_3OZn$	$C_{16}H_{21}Cl_2N_3OZn$	$C_{32}H_{42}Cl_2N_6O_{10}Zn$
Formula weight	393.62	407.65	807.00
Crystal system	triclinic	monoclinic	orthorhombic
Space group	$P\bar{1}$	$P2_1/n$	*Pbcn*
a (Å)	7.4162(8)	8.0633(5)	20.308(3)
b (Å)	8.6223(10)	8.8955(6)	10.6095(18)
c (Å)	14.2351(18)	25.1516(17)	17.139(3)
α (°)	82.875(4)	90	90
β (°)	81.916(4)	96.411(4)	90
γ (°)	68.504(3)	90	90
V (Å^3)	835.93(17)	1792.8(2)	3692.8(11)
Z	2	4	4
D_{calc} (g cm^{-3})	1.564	1.510	1.451
μ (cm^{-1})	17.924	16.744	8.722
$2\theta_{max}$ (°)	55.0	55.0	57.4
T (K)	173	123	173
Number of reflections collected	6445	17 201	29 575
Number of reflections used	3645	4111	4736
Number of parameters	276	293	232
Final R_1 ($I > 2\theta(I)$)	0.0209	0.0324	0.0411
wR_2 (all data)	0.0560	0.0991	0.1092
Goodness-of-fit (GOF)	1.042	1.077	1.058

$R_1 = (\sum ||F_o| - |F_c||)/(\sum |F_o|)$. $wR_2 = \{[\sum w(F_o^2 - F_c^2)^2]/[\sum w(F_o^2)^2]\}^{1/2}$.

Table 2
Crystallographic data for [Zn($\mathbf{L}^{Py}$)Cl](ClO$_4$) (**4**) and [Zn($\mathbf{L}^{Py}$)Br](ClO$_4$) (**5**).

	[Zn($\mathbf{L}^{Py}$)Cl](ClO$_4$) (**4**)	[Zn($\mathbf{L}^{Py}$)Br](ClO$_4$) (**5**)
Formula	$C_{21}H_{24}Cl_2N_4O_5Zn$	$C_{21}H_{24}BrClN_4O_5Zn$
Formula weight	548.73	593.18
Crystal system	monoclinic	monoclinic
Space group	$P2_1/c$	$P2_1/c$
a (Å)	12.7997(4)	13.009(3)
b (Å)	10.6600(3)	10.573(2)
c (Å)	16.6604(6)	16.811(3)
β (°)	98.7858(19)	97.681(3)
V (Å^3)	2246.55(12)	2291.3(8)
Z	4	4
D_{calc} (g cm^{-3})	1.622	1.719
μ (cm^{-1})	13.733	29.793
$2\theta_{max}$ (°)	55.0	55.0
T (K)	123	123
Number of reflections collected	17 132	17 484
Number of reflections used	5135	5125
Number of parameters	395	395
Final R_1 ($I > 2\theta(I)$)	0.0340	0.0299
wR_2 (all data)	0.0898	0.0748
Goodness-of-fit (GOF)	1.094	1.070

$R_1 = (\sum ||F_o| - |F_c||)/(\sum |F_o|)$. $wR_2 = \{[\sum w(F_o^2 - F_c^2)^2]/[\sum w(F_o^2)^2]\}^{1/2}$.

^{1}H NMR (CD$_3$OD): δ 8.72 (d, J = 5.4 Hz, 2H), 8.20 (ddd, J = 1.8, 7.8, 7.8 Hz, 2H), 7.7–7.8 (m, 4H), 4.51 (d, J = 16.5 Hz, 2H), 4.19 (d, J = 16.5 Hz, 2H), 3.40 (t, J = 5.7 Hz, 2H), 3.28 (s, 3H), 2.73–2.79 (m, 2H), 1.8–2.0 (m, 2H).

^{13}C NMR (CD$_3$OD): δ 156.5, 149.0, 142.6, 126.4, 126.2, 71.8, 59.0, 58.4, 52.6, 24.0.

Anal. Calc. for $C_{32}H_{42}Cl_2N_6O_{10}Zn$ (**3**): C, 47.63; H, 5.25; N, 10.41. Found: C, 47.76; H, 5.43; N, 10.11%.

*2.2.2.4. [Zn($\mathbf{L}^{Py}$)Cl](ClO$_4$) (**4**).* Methanolic solution (0.2 mL) of $\mathbf{L}^{Py}$ (24.4 mg, 0.070 mmol) was mixed with ZnCl$_2$ (9.5 mg, 0.070 mmol) in the same solvent (0.2 mL) at room temperature. Then, NaClO$_4$·H$_2$O (9.8 mg, 0.070 mmol) in the same solvent (0.1 mL) was added and ether vapor was introduced at 4 °C. After 1 day, single crystals suitable for X-ray crystallography were obtained directly from the reaction mixture (16.2 mg, 0.030 mmol, 42% yield). Table 2 summarizes the crystallographic parameters.

^{1}H NMR (CD$_3$OD): δ 9.33 (br., 1H), 8.31 (br., 1H), 8.03–8.3 (m, 2H), 7.74–7.81 (br., 4H), 7.45–7.62 (br., 2H), 7.42–7.45 (br., 2H), 4.74 (d, J = 11.7 Hz, 2H), 4.64 (br., 1H), 4.32 (d, J = 11.7 Hz, 2H), 3.53–3.56 (br., 2H), 2.96–2.99 (br., 2H), 1.34–1.36 (br., 2H).

^{13}C NMR (CD$_3$OD): δ 156.3, 150.0, 147.2, 142.1, 141.5, 125.9, 125.8, 125.2, 124.1, 74.8, 71.4, 63.1, 60.8, 26.6.

Anal. Calc. for $C_{21}H_{24}Cl_2N_4O_5Zn$ (**4**): C, 45.96; H, 4.41; N, 10.21. Found: C, 45.83; H, 4.43; N, 10.11%.

*2.2.2.5. [Zn($\mathbf{L}^{Py}$)Br](ClO$_4$) (**5**).* Methanolic solution (0.4 mL) of $\mathbf{L}^{Py}$ (17.4 mg, 0.050 mmol) was mixed with ZnBr$_2$ (11.2 mg, 0.050 mmol) in the same solvent (0.4 mL) at room temperature. Then, ether vapor was introduced at 4 °C. The appeared precipitate was removed by filtration. To the filtrate, NaClO$_4$·H$_2$O (14.0 mg, 0.10 mmol) was added and ether vapor was introduced at 4 °C. After 2 days, single crystals suitable for X-ray crystallography were obtained (18.5 mg, 0.031 mmol, 62% yield). Table 2 summarizes the crystallographic parameters.

^{1}H NMR (CD$_3$OD): δ 9.48 (d, J = 5.4 Hz, 1H), 8.34 (dd, J = 7.8, 7.8 Hz, 1H), 8.11 (dd, J = 7.8, 7.8 Hz, 2H), 7.69–7.9 (m, 4H), 7.70 (d, J = 7.8 Hz, 2H), 7.46–7.54 (m, 2H), 4.98 (s, 2H), 4.84 (d, J = 15.6 Hz, 2H), 4.37 (d, J = 15.6 Hz, 2H), 3.61 (t, J = 5.1 Hz, 2H), 3.02–3.06 (m, 2H), 1.35–1.48 (m, 2H).

^{13}C NMR (CD$_3$OD): δ 157.3, 156.5, 150.6, 147.4, 142.4, 141.8, 126.1, 125.5, 124.4, 75.0, 71.5, 62.9, 60.7, 26.5.

Anal. Calc. for $C_{21}H_{24}BrClN_4O_5Zn$ (**5**): C, 42.52; H, 4.08; N, 9.45. Found: C, 42.28; H, 4.08; N, 9.33%.

2.3. X-ray crystallography

Single crystals of **1–5** were covered by paraffin oil and mounted on a glass fiber. All data were collected at 123 or 173 K on a Rigaku Mercury CCD detector, with monochromatic MoKα radiation, oparating at 50 kV/40 mA. Data were processed on a PC using CrystalClear Software (Rigaku). Structures were solved by direct methods (SIR-92) [33] and refined by full-matrix least-squares methods on F^2 (SHELXL-97) [34].

3. Results and discussion

3.1. Preparation and structure determination of complexes

Single crystals of complexes **1–5** were prepared from methanol solutions of ligand and metal salts in some cases under slow ether diffusion conditions in the presence of sodium perchlorate. Crystallographic data and X-ray diffraction conditions are summarized in Tables 1 and 2. ORTEP diagrams of complexes **1–5** are shown in Figs. 1, 2 and 5–7. Selected bond distances were listed in Table 3.

All solved structures exhibit meridional coordination geometries for the DPA moiety [5–9,11,35,36]. The complexes, [Zn(**L**)Cl$_2$] (**1**), [Zn($\mathbf{L}^{Py}$)Cl](ClO$_4$) (**4**), and [Zn($\mathbf{L}^{Py}$)Br](ClO$_4$) (**5**), exhibit the coordination of the ether oxygen atom to the zinc center with Zn–O bond lengths between 2.2742 and 2.6384 Å.

3.2. *L* and *L′* complexes

Zinc chloride complexes with **L** and **L′** both afforded single crystals suitable for X-ray crystallography (Figs. 1 and 2). The number of atoms in chelate chain differentiates the coordination of the ether oxygen atom. The metal–oxygen interaction affording a five-membered chelate ring in **L**–ZnCl$_2$ complex (**1**) is no more available in **L′**–ZnCl$_2$ complex (**2**), in which six-membered chelate ring would be formed when the ether oxygen atom coordinates to the metal center. Complex **1** has two coordinated chloride anions that cancel out the complex charge, thus the neutral nature of the complex have a weak ability to form metal–ether oxygen bond and no examples are found for zinc complexes having three nitrogens, two halogens, and metal-bound ether oxygen atoms in the crystal structure. Most of such a $N_3O_1X_2$ (X: halogen) system in Cu/Zn complex includes phenol [37–39] or alcohol [40,41] moiety as an oxygen donor. Only one example was found for copper complex in $N_3O(ether)_1X_2$ coordination environment [42].

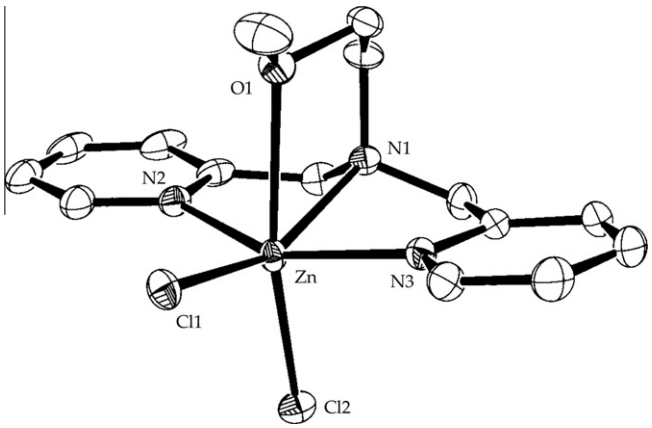

Fig. 1. ORTEP for [Zn(**L**)Cl$_2$] (**1**) (50% probability).

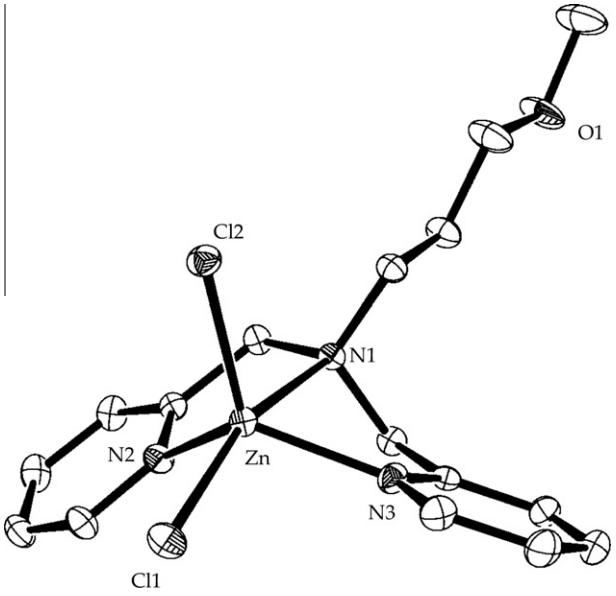

Fig. 2. ORTEP for [Zn(**L**′)Cl$_2$] (**2**) (50% probability).

The coordination structure of the complexes was further investigated by ^{1}H NMR spectroscopy in methanol solution (Figs. 3 and 4). Upon addition of $ZnCl_2$ into CD_3OD solution of **L**, a new set of signals assigned to the zinc complex was appeared (Fig. 3). The chemical shifts for the proton signals of remaining free ligand were unchanged during the titration, indicating that the metal exchange between Zn-complex and free ligand is slow compared with NMR timescales. Although most of signals from Zn-complex appear in the downfield region compared to those of free ligand, the methylene (CH_2-3) and methyl (CH_3-4) groups neighboring to the ether oxygen atom exhibit upfield shift ($\Delta_{ppm} = -0.5$ for CH_2-3 and -0.1 for CH_3-4). This is because the ether oxygen-coordinated structure elucidated by the crystallography ([Zn(**L**)Cl$_2$] (**1**), Fig. 1) is preserved in the methanol solution and the ring current effect from the pyridine ring causes the upfield shift of those proton signals. On the other hand, proton signals in ether side chain of the [Zn(**L**′)Cl$_2$] complex exhibited negligible metal-induced chemical shift change (Fig. 4, $\Delta_{ppm} = +0.25$, -0.03, -0.06, and $+0.04$ for CH_2-2, 3, 4, and CH_3-5, respectively), indicating that the ether oxygen is not coordinated to the zinc center as found in the crystal structure (Fig. 2). Here again, the numbers of chelating atoms determines the ether oxygen coordination.

For the preparation of zinc complex with **L**′, replacement of chloride with perchlorate would yield the cationic complexes that tend to have ether oxygen-coordinated species because the coordination ability of perchlorate is weak [10]. The methanol solution of **L**′ in the presence of $Zn(ClO_4)_2$ afforded [Zn(**L**′)$_2$](ClO$_4$)$_2$ (**3**), in which six nitrogen atoms of *cis*-orientated two ligand molecules coordinated to the zinc center even in the presence of 1 eq of ligand (Fig. 5). The formation of this complex may be a crystallization effect, however, 40% isolated yield of this complex and ^{1}H NMR spectrum of **L**′ in the presence of 1 eq. of $Zn(ClO_4)_2$ in CD_3OD (data not shown) strongly discourages the coordination of the ether oxygen atom of **L**′. In spite of extensive crystallization trials, the mixture of **L** and $Zn(ClO_4)_2$ in methanol did not afford single crystals suitable for X-ray crystallography.

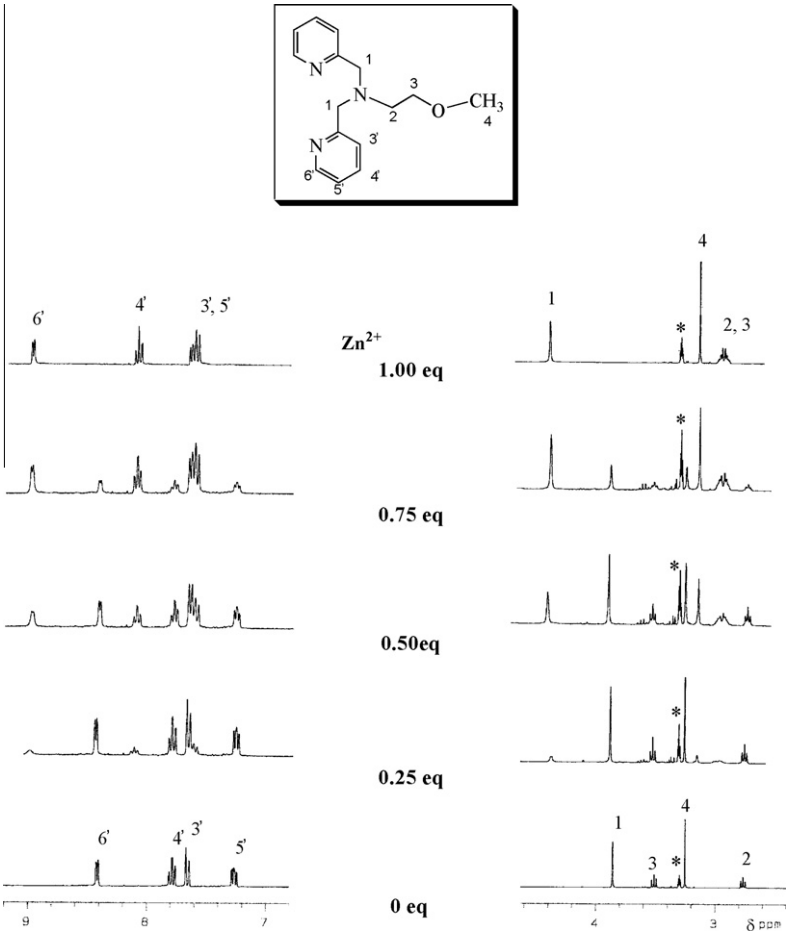

Fig. 3. Zn^{2+}-induced ^{1}H NMR spectral changes of **L** in the presence of increasing amount of $ZnCl_2$ in CD_3OD. Asterisk indicates solvent peak.

Table 3
Bond lengths around zinc center in complexes **1**–**5**.

Complex	Zn–N1	Zn–N2	Zn–N3	Zn–X_{basal}	Zn–O1	Zn–X_{ap}
[Zn(**L**)Cl_2] (**1**)	2.2846(11)	2.1226(13)	2.1398(11)	2.2889(3)[a]	2.6384(10)	2.3599(3)[a]
[Zn(**L**′)Cl_2] (**2**)	2.3857(18)	2.0879(18)	2.082(2)	2.3234(5)[a]		2.2696(6)[a]
[Zn(**L**′)$_2$]$(ClO_4)_2$ (**3**)	2.3045(16)	2.1206(16)	2.1793(18)			
[Zn($\mathbf{L}^{Py}$)Cl](ClO_4) (**4**)	2.2042(16)	2.1740(15)	2.1134(16)	2.0963(15)[b]	2.2784(14)	2.3458(5)[a]
[Zn($\mathbf{L}^{Py}$)Br](ClO_4) (**5**)	2.2056(17)	2.1098(16)	2.1704(16)	2.1011(16)[b]	2.2742(15)	2.5110(3)[c]

[a] X = Cl.
[b] X = N.
[c] X = Br.

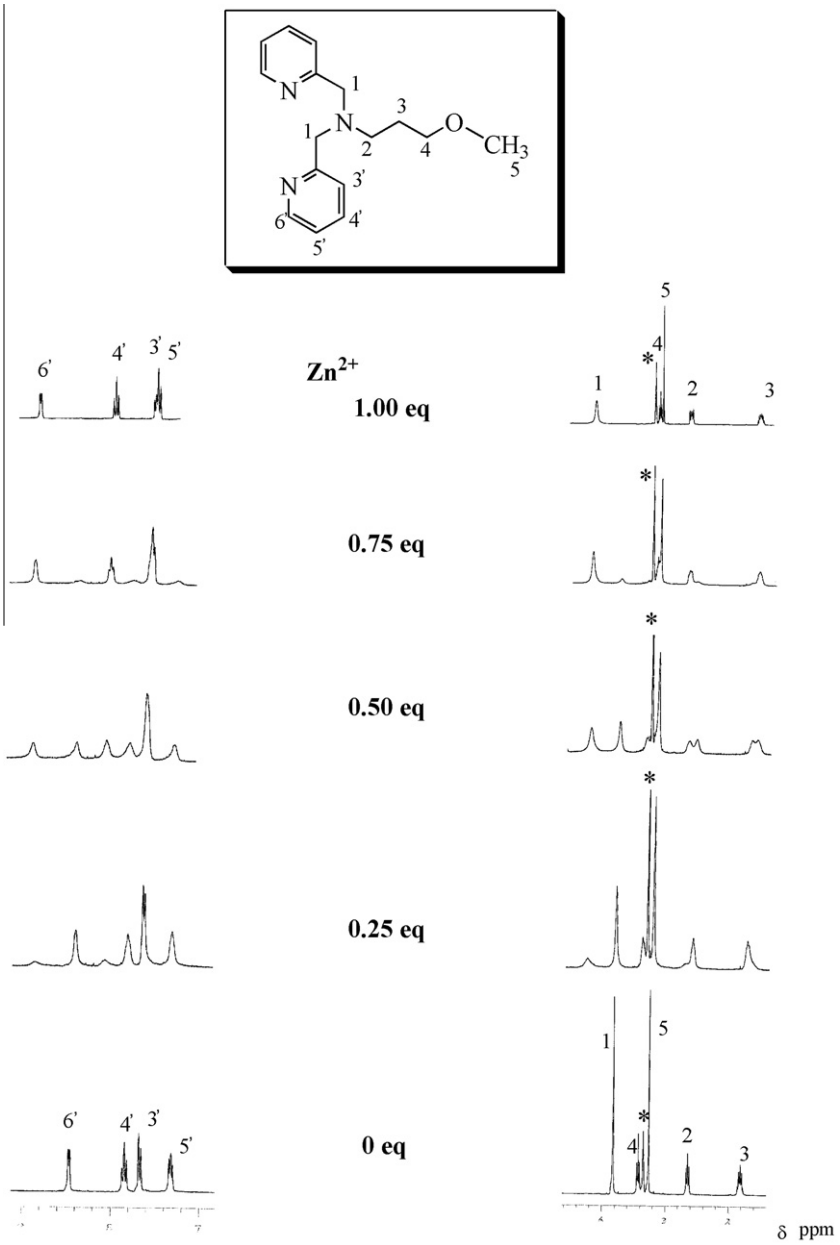

Fig. 4. Zn^{2+}-induced ^{1}H NMR spectral changes of **L**′ in the presence of increasing amount of $ZnCl_2$ in CD_3OD. Asterisk indicates solvent peak.

3.3. $\boldsymbol{L^{Py}}$ complexes

Previous works revealed that anchoring group such as hydroxyl group facilitates the ether oxygen coordination [10,43]. In this work, a hydrogen atom in the methyl group of **L**′ was replaced with 2-pyridyl group to promote the coordination of ether oxygen atom, in which six- and five-membered chelate ring would be formed around 3-aminopropyl 2-pyridylmethyl ether moiety.

The ligand $\mathbf{L}^{Py}$ was prepared from *N*,*N*-bis(2-pyridylmethyl)-3-aminopropanol and 2-pyridylmethyl chloride. The zinc complexes

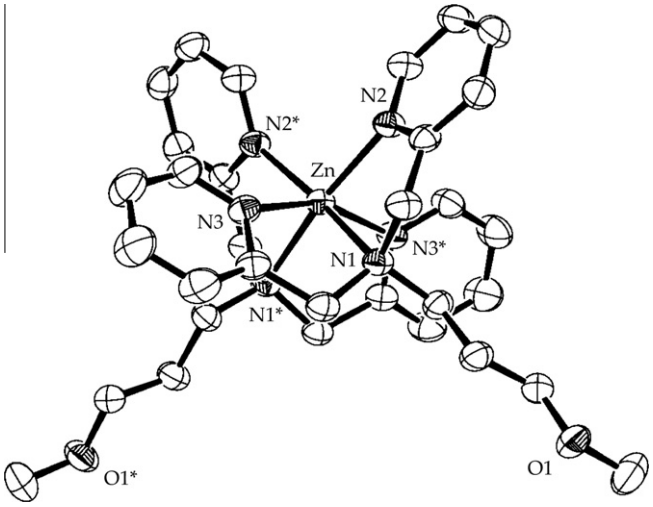

Fig. 5. ORTEP for cationic portion of $[Zn(\mathbf{L}')_2](ClO_4)_2$ (**3**) (50% probability). Atoms generated by symmetric operation are indicated with an asterisk.

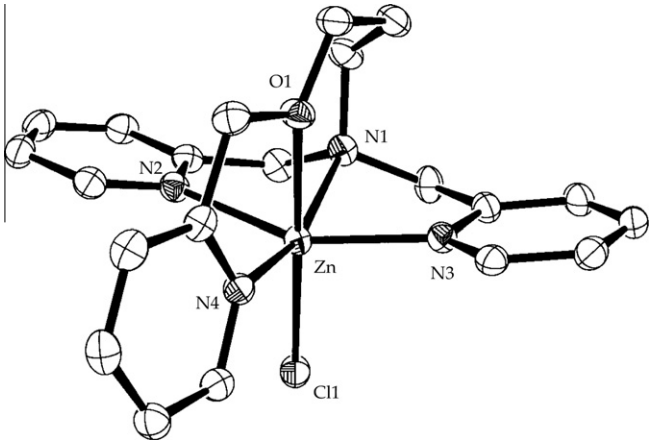

Fig. 6. ORTEP for cationic portion of $[Zn(\mathbf{L}^{Py})Cl](ClO_4)$ (**4**) (50% probability).

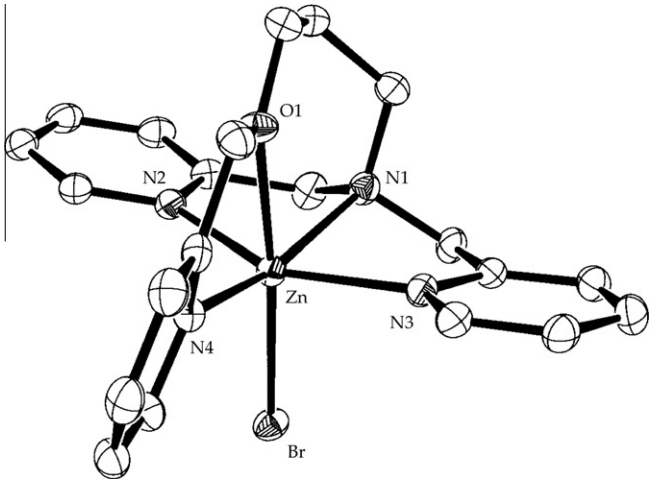

Fig. 7. ORTEP for cationic portion of $[Zn(\mathbf{L}^{Py})Br](ClO_4)$ (**5**) (50% probability).

with $\mathbf{L}^{Py}$ were prepared with $ZnCl_2$ ($[Zn(\mathbf{L}^{Py})Cl](ClO_4)$, **4**) and $ZnBr_2$ ($[Zn(\mathbf{L}^{Py})Br](ClO_4)$, **5**) with the help of sodium perchlorate, and were characterized with X-ray crystallography (Figs. 6 and 7) and elemental analysis. No complex was isolated from the reaction mixture in methanol in the absence of sodium perchlorate.

The $\mathbf{L}^{Py}$ complexes **4** and **5** exhibited their ether oxygen atom bound to the metal center. The Zn–O distances are 2.2784(14) and 2.2742(15) Å for complexes **4** and **5**, respectively. These distances are significantly shorter than that of complex **1** (2.6384(10) Å) by the effect of anchoring pyridine group. The steric hindrance of chloride and bromide in complexes **4** and **6** tilts the anchor pyridine ring, resulting a significant distortion of aminopropyleneoxy chelate ring.

4. Conclusion

The intramolecular ether oxygen coordination to the metal center is strongly perturbed by the ligand structure. In this article, the first example of crystal structure of $ZnN_3X_2O_{ether}$ (X = halogen) system ($[Zn(\mathbf{L})Cl_2]$, **1**) is presented. Generally, complexes that have positive charge exhibit coordination of the ether oxygen atom, whereas chargeless complexes in which two anions are bound to the metal center ligated by a neutral ligand tend to dissociate the ether oxygen. The five-membered chelate ring formation could hold the ether oxygen coordination in complex **1**. On the other hand, the six-membered chelate ring of $\mathbf{L}'$ is disfavored and zinc does not coordinate to the oxygen in complex **2** in both solid and solution. Additional metal binding site, namely pyridine moiety in $\mathbf{L}^{Py}$, promotes the formation of six-membered ring containing the ether oxygen coordination. Weak coordinating ability of perchlorate yields the ML_2 type complex ($[Zn(\mathbf{L}')_2](ClO_4)_2$, **3**) without ether oxygen coordination. The present information provides important information about the coordination of oxygen atom to the metal center in the solid and solution state.

Acknowledgements

This work was supported by the Asahi-Glass Foundation, Nara Women's University Intramural Grant for Project Research, and Grant-in Aid for Scientific Research from the MEXT, Japan (18550059 and 20550065).

Appendix A. Supplementary material

CCDC 779482, 779483, 779484, 779485 and 779487 contain the supplementary crystallographic data for this paper. These data can be obtained free of charge from The Cambridge Crystallographic Data Centre via www.ccdc.cam.ac.uk/data_request/cif. Supplementary data associated with this article can be found, in the online version, at doi:10.1016/j.ica.2011.02.022.

References

[1] J.D. Badjic, A. Nelson, S.J. Cantrill, W.B. Turnbull, J.F. Stoddart, Acc. Chem. Res. 38 (2005) 723.
[2] G.W. Gokel, Chem. Soc. Rev. (1992) 39.
[3] G.W. Gokel, W.M. Leevy, M.E. Weber, Chem. Rev. 104 (2004) 2723.
[4] H. An, J.S. Bradshaw, R.M. Izatt, Chem. Rev. 92 (1992) 543.
[5] M.J. Young, D. Wahnon, R.C. Hynes, J. Chin, J. Am. Chem. Soc. 117 (1995) 9441.
[6] M. Palaniandavar, R.J. Butcher, A.W. Addison, Inorg. Chem. 35 (1996) 467.
[7] M. Palaniandavar, S. Mahadevan, M. Köckerling, G. Henkel, J. Chem. Soc., Dalton Trans. (2000) 1151.
[8] T. Murakami, S. Hatakeyama, S. Igarashi, Y. Yukawa, Inorg. Chim. Acta 310 (2000) 96.
[9] F. Ugozzoli, C. Massera, A. Maria, M. Lanfredi, N. Marsich, A. Camus, Inorg. Chim. Acta 340 (2002) 97.
[10] Y. Mikata, T. Fujimoto, Y. Sugai, S. Yano, Eur. J. Inorg. Chem. (2007) 1143.
[11] S.I. Kirin, P. Dübon, T. Weyhermüller, E. Bill, N. Metzler-Nolte, Inorg. Chem. 44 (2005) 5405.
[12] Y. Mikata, Y. Sugai, S. Yano, Inorg. Chem. 43 (2004) 4778.
[13] Y. Mikata, Y. Sugai, M. Obata, M. Harada, S. Yano, Inorg. Chem. 45 (2006) 1543.
[14] H. Sigel, L.E. Kapinos, Coord. Chem. Rev. 200–202 (2000) 563.
[15] H. Sigel, Chem. Soc. Rev. 33 (2004) 191.

[16] B.L. Vallee, K.H. Falchuk, Physiol. Rev. 73 (1993) 79.
[17] B.L. Vallee, D.S. Auld, Acc. Chem. Res. 26 (1993) 543.
[18] K. Komatsu, K. Kikuchi, H. Kojima, Y. Urano, T. Nagano, J. Am. Chem. Soc. 127 (2005) 10197.
[19] N.C. Lim, J.V. Schuster, M.C. Porto, M.A. Tanudra, L. Yao, H.C. Freake, C. Brückner, Inorg. Chem. 44 (2005) 2018.
[20] L. Xue, H.-H. Wang, X.-J. Wang, H. Jiang, Inorg. Chem. 47 (2008) 4310.
[21] B.A. Wong, S. Friedle, S.J. Lippard, J. Am. Chem. Soc. 131 (2009) 7142.
[22] B. Bauer-Siebenlist, F. Meyer, E. Farkas, D. Vidovic, S. Dechert, Chem. Eur. J. 11 (2005) 4349.
[23] N. Niklas, O. Walter, R. Alsfasser, Eur. J. Inorg. Chem. (2000) 1723.
[24] G. Parkin, Chem. Commun. (2000) 1971.
[25] M. Livieri, F. Mancin, U. Tonellato, J. Chin, Chem. Commun. (2004) 2862.
[26] C. Liu, M. Wang, T. Zhang, H. Sun, Coord. Chem. Rev. 248 (2004) 147.
[27] A. Ojida, H. Nonaka, Y. Miyahara, S. Tamaru, K. Sada, I. Hamachi, Angew. Chem., Int. Ed. 45 (2006) 5518.
[28] H.K. Cho, D.H. Lee, J.-I. Hong, Chem. Commun. (2005) 1690.
[29] D.H. Lee, S.Y. Kim, J.-I. Hong, Angew. Chem., Int. Ed. 43 (2004) 4777.
[30] A. Ojida, I. Takashima, T. Kohira, H. Nonaka, I. Hamachi, J. Am. Chem. Soc. 130 (2008) 12095.
[31] A. Ojida, M. Inoue, Y. Moto-oka, H. Tsutsumi, K. Sada, I. Hamachi, J. Am. Chem. Soc. 128 (2006) 2052.
[32] J.-Z. Wu, E. Bouwman, A.M. Mills, A.L. Spek, J. Reedijk, Inorg. Chim. Acta 357 (2004) 2694.
[33] SIR-92 A. Altomare, G. Cascarano, C. Giacovazzo, A. Guagliardi, M.C. Burla, G. Polidori, M. Camalli, J. Appl. Crystallogr. 27 (1994) 435.
[34] G.M. Sheldrick, SHELXL-97, Program for refinement of crystal structures, University of Göttingen, Germany, 1997.
[35] Y. Ishikawa, S. Ito, S. Nishino, S. Ohba, Y. Nishida, Z. Naturforsch, C: Biosciences 53 (1998) 378.
[36] S. Tanase, C. Foltz, R. de Gelder, R. Hage, E. Bouwman, J. Reedijk, J. Mol. Catal. A: Chem. 225 (2005) 161.
[37] M.C.B. de Oliveira, M. Scarpellini, A. Neves, H. Terenzi, A.J. Bortoluzzi, B. Szpoganics, A. Greatti, A.S. Mangrich, E.M. de Souza, P.M. Fernandez, M.R. Soares, Inorg. Chem. 44 (2005) 921.
[38] A. Philibert, F. Thomas, C. Philouze, S. Hamman, E. Saint-Aman, J.-L. Pierre, Chem. Eur. J. 9 (2003) 3803.
[39] I.A. Koval, M. Sgobba, M. Huisman, M. Lüken, E. Saint-Aman, P. Gamez, B. Krebs, J. Reedijk, Inorg. Chim. Acta 359 (2006) 4071.
[40] A. Nielsen, S. Veltzé, A.D. Bond, C.J. McKenzie, Polyhedron 26 (2007) 1649.
[41] P.J. van Koningsbruggen, J.W. van Hal, R.A.G. de Graaff, J.G. Haasnoot, J. Chem. Soc., Dalton Trans. (1993) 2163.
[42] G.R. Newkome, Y.J. Joo, D.W. Evans, F.R. Fronczek, G.R. Baker, J. Org. Chem. 55 (1990) 5714.
[43] S.I. Kirin, C.M. Happel, S. Hrubanova, T. Weyhermüller, C. Klein, N. Metzler-Nolte, Dalton Trans. (2004) 1201.